Note

CO_2 storage capacity subject to geological uncertainty

Contributions to CLIMIT research project
"Geological Storage of CO2:
Mathematical Modelling and Risk Analysis"

Note no	**SAND/02/2010**
Authors	**Arne Skorstad**
Date	**February 2010**

About the authors

Arne Skorstad is the assistant research director at the SAND department at Norwegian Computing Center.

Norsk Regnesentral

Norsk Regnesentral (Norwegian Computing Center, NR) is a private, independent, non-profit foundation established in 1952. NR carries out contract research and development projects in the areas of information and communication technology and applied statistical modelling. The clients are a broad range of industrial, commercial and public service organizations in the national as well as the international market. Our scientific and technical capabilities are further developed in co-operation with The Research Council of Norway and key customers. The results of our projects may take the form of reports, software, prototypes, and short courses. A proof of the confidence and appreciation our clients have for us is given by the fact that most of our new contracts are signed with previous customers.

The project was carried out in close cooperation with both the SINTEF ICT research group and the department of Mathematics at the University of Bergen, both Norway.

Title	**CO_2 storage capacity subject to geological uncertainty**
Authors	**Arne Skorstad**
Date	February 22
Year	2010
Publication number	SAND/02/2010

Abstract

Realistic synthetic reservoir realizations generated in the SAIGUP project are reused in a project investigating and quantifying the effect of CO_2 injection in realistic heterogeneous reservoir as opposed to homogeneous reservoirs.

The reservoirs described in this note have been transferred to the project partner SINTEF ICT, where CO_2 injectivity simulations are carried out.

Contents

List of figures

Figure 8. The mapping process from a structurally unfaulted geostatistical fine scale domain into the synthetic fine scale reservoir is shown. Each, in this case, SATNUM value is I,J,K-sampled

NR **CO2 storage capacity subject to geological uncertainty**

1   Introduction

There is a need for quantifying the effect of CO_2 injection in heterogeneous reservoirs, and compare this with the injectivity in homogeneous reservoirs, where analytical calculations are conducted, and documented in the literature. This note describes the contribution by NR into a CLIMIT supported research project "Geological Storage of CO_2: Mathematical Modelling and Risk Analysis (178013)" (MatMoRA). The MatMoRA project aims to develop analytical and numerical tools to be used in risk assessment analysis of geological storage of CO_2. The flow simulations of the reservoirs have been made at SINTEF ICT. The results of these are not included in this note, which only covers the input realizations.

The main purpose of this note is to document which of the original SAIGUP realizations that was used in the numerical CO_2 injection tests at SINTEF. A full tabular overview is found in Table 2.

2   The synthetic reservoir realizations

NR was a partner in the EU-supported project SAIGUP (contract number ENK6 – CT – 2000 – 00073), run in 2000-2003. Here, a large number of realistic, synthetic reservoirs were generated for the shallow marine class of reservoirs. The methodology and results of that project have been published in several articles in a special publication of the Petroleum Geoscience journal (Petr. Geosci. Vol. **14**, No 1. 2008). The rationale and choices of geological heterogeneity were thoroughly described in the publications. This basis made it natural to adopt synthetic reservoir realizations from the SAIGUP study also to investigate on the CO_2 injectivity in heterogeneous reservoirs. Although synthetic reservoirs from the SAIGUP domain does not include all classes of possible storage reservoirs for injected CO_2, the present study demonstrates a methodology which is valid for a wider class of sedimentological scenarios. The purpose of the project cooperation between NR and SINTEF is to investigate and quantify the effect of heterogeneity on CO_2 injection in stochastically generated reservoirs and compare with numerical and analytical studies on homogeneous reservoirs where injected CO_2 creates a perfect plume shape.

2.1   Unfaulted realizations

The SAIGUP reservoirs are 3 km by 9 km laterally and 80 m thick. The overall structure is depicted in Figure 1, and shows the structural trap limited by aquifer to the north, west and south, and a major fault to the eastern crest.

All cells east of the main fault are non-active cells (given by the ACTNUM keyword in ECLIPSE format).
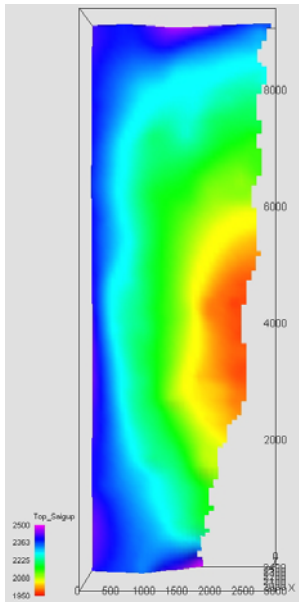
Figure 1. Structural overview of the SAIGUP reservoirs, showing top map of non-faulted realizations.

The reservoirs are filled with rock properties based on the sedimentological and petrophysical heterogeneity. In the SAIGUP domain of reservoirs, four sedimentological parameters were varied stochastically within three different parameter groups. These were:

- Progradation direction relative to the dipping structure.

- Aggradation angle, controlling the ratio between the sediment supply and the change in sea level. This parameter can be considered as the vertical angle of the continuity of the sedimentological facies.

- Barriers on the flow both laterally and vertically, as 10%, 50% or 90% barrier coverage.

- Lobosity, determining the lateral heterogeneity arising from the ratio between the sediment supply and the available accommodation space in the sea.

More details are found in Howell *et al*. 2008.

In the SAIGUP study, the progradation of the distributary system was changed between three different directions. In this CO_2 storage setting where only injection from one well is investigated, we only use two of these, being progradation up-dip of down-dip. The aggradation and barrier parameters are exemplified in Figure 2, while the three different progradation sets, for the up-dip case, are given in Figure 3.
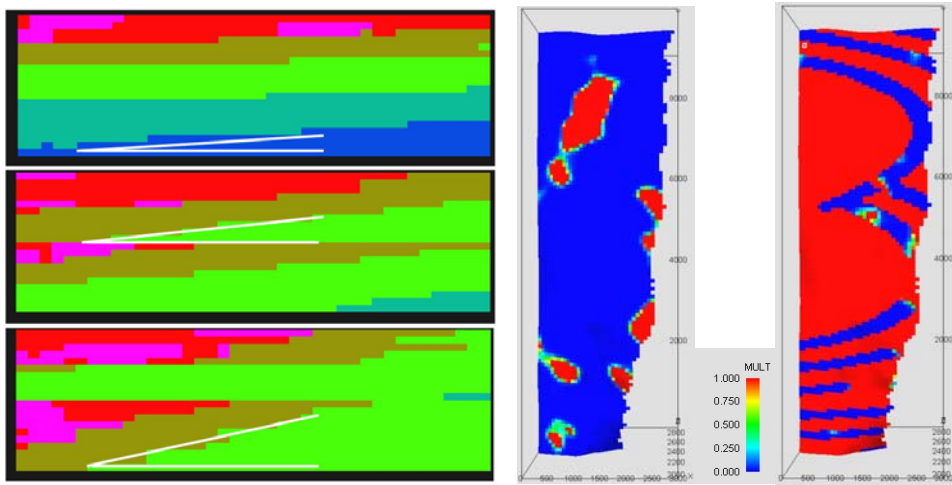
Figure 2. Aggradation angle increasing from top to bottom in side view pictures (left), and multiplicator representing vertical barriers between two major subzones (middle) and vertical and horizontal barriers in a two-lobe up-dip progradational system (right).
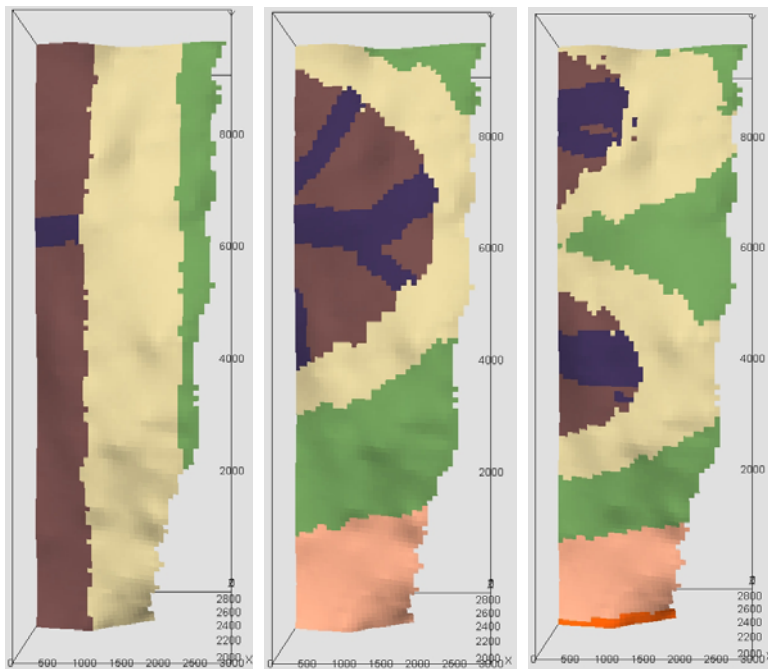
Figure 3. Parallel shorefront (left), and one (middle) and two (right) shore front lobes shown in top view.

The reservoirs were generated from 3 aggradation angles * 3 barrier levels * 3 shorefront shapes * 2 progradation directions, giving in total 54 stochastically generated synthetic reservoirs used as test reservoir for CO_2 injection.

2.2 Faulted realizations

Several structural fault scenarios were included in the SAIGUP study. Only one of these was included in this study in addition to the non-faulted case. The structural outline is shown in Figure 4. The faults are seen to run along the main outline of the reservoir, and will be barriers for flow towards the top of the structure. However, the faults will also imply a wider spread of

flow. The effective fault permeability of all fault scenarios is depending on the Shale Gouge Ratio, which again depends on the amount of clay in each cell. The fault case from SAIGUP that was used here (A23) had a fault permeability higher than the average among those tested in SAIGUP. The key objective in this study is, however, to investigate on a more quantitative manner if faults do affect CO_2 injectivity. It has therefore not been any effort to optimize the fault scenario chosen here.
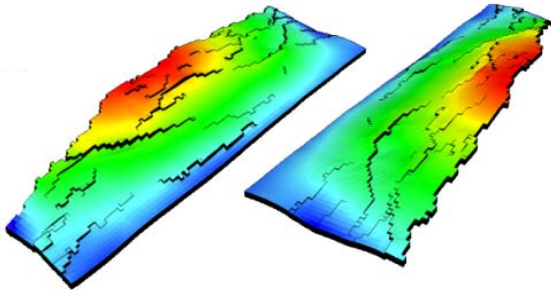
Figure 4. Structural outline of faulted case is shown from two angles. Faults run predominantly along the reservoir.

All 54 non-faulted reservoir realizations are repeated with respect to cell content of all parameters. In addition, non-neighbouring connections (NNC's) are added, and the geometric locations of the cells are shifted due to the faulting. Thereby, there is straightforward to investigate the effect of the fault compared to the non-faulted case.

3 Pore volume heterogeneity

Since the reservoirs are stochastically generated, they will not be exactly similar with respect to petrophysical properties. The pore volume distribution is shown in Figure 5.
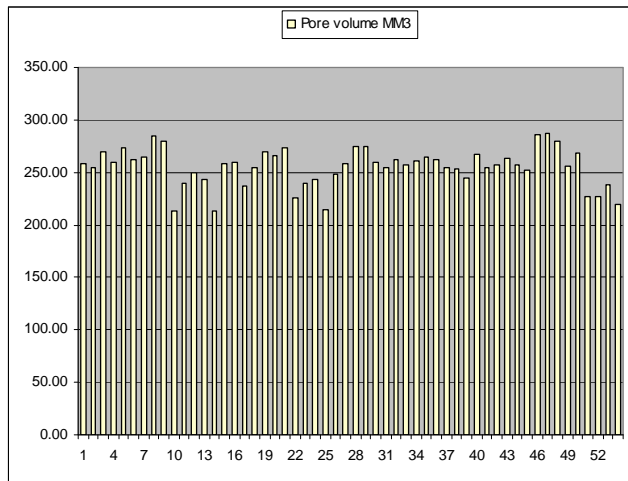
Figure 5. Pore volumes of 54 non-faulted realizations used in CO_2 injection study.

The mean pore volume is 255.2 million cubic meters (MM3), with a standard deviation of 18.1 MM3. Sorting the pore volumes and identifying them with the two progradation directions gives Figure 6.
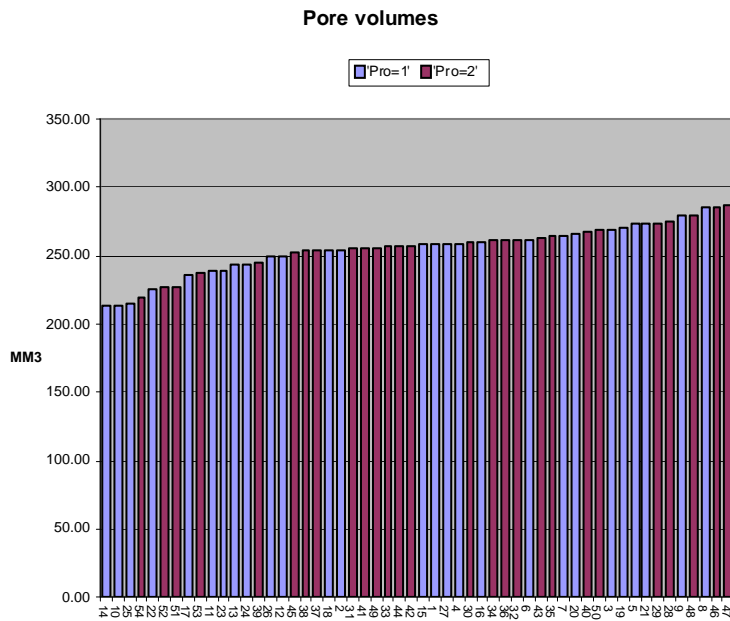
Pore volumes

Figure 6. Pore volume dependency of progradation direction. Progradation equal to "1" indicates up-dip and "2" down-dip, respectively.

Similarly, colouring the pore volumes dependency on the aggradation and the lobosity produces Figure 7.
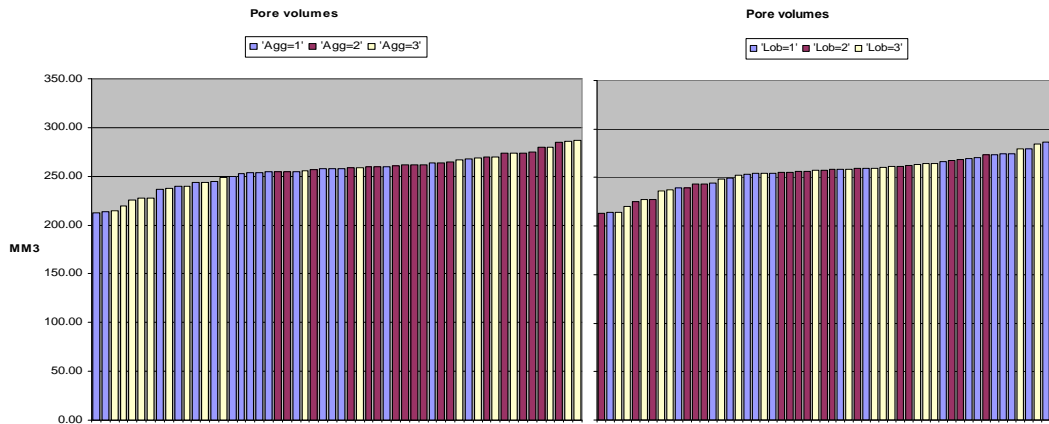
Figure 7. Pore volume dependency of aggradation (left) and lobosity (right). Aggradation equal to "1" indicates low, "2" for medium and "3" for high angle, respectively. Lobosity equal to "1" indicates parallel shoreface, "2" for 1 lobe and "3" for 2 lobes, respectively.

The differences shown in Figure 6 and Figure 7 are also quantified in tabular form in Table 1.

Group	Progradation		Aggradation			Shoreface		
Parameter level	Up-dip	Down-dip	Low	Medium	High	Parallel	1 lobe	2 lobes
Mean	252.4	257.9	248.5	265.3	251.8	261.6	251.4	252.6
Std.dev	19.6	16.4	15.0	8.8	23.4	18.2	16.2	18.9

Table 1. Pore volumes as a function of primary parameter level. All values in million cubic meters.

The main observation is that the differences are largest for the aggradation angle. Especially for the medium aggradation, the pore volumes are significantly higher than both the low and the high angle case. This is a consequence of the stochastically generation of the reservoir, not intended, but important to consider when analyzing the results of the CO_2 injection studies.

Progradation and shoreface shape do not exhibit large differences, and the barrier levels should neither, as the multiplicators are not volumetric entities.

4 Fine scale realization

All the realizations described earlier have been on a 40*120*20 grid. These have all been obtained from upscaling from an 80*240*80 fine scale grid where the geological realizations are constructed.

It was decided to generate also one fine scale realization. The rationale was to be able to investigate the effect from the grid scale and upscaling on the CO_2 injectivity. The unfaulted realization number 35 in the original SAIGUP suite was chosen, by random. The top and bottom structural maps were only available on the coarse scale. Therefore, the values from the original detailed geostatistical resolution were mapped into a new grid generated by sampling the coarse scale map values into the finer, more detailed scale. Laterally, this means that each coarse scale cell was the mother of 4 fine scale structural map values. The resampling procedure shown in Figure 8 for one cell was repeated for all cells in the fine scale representation.
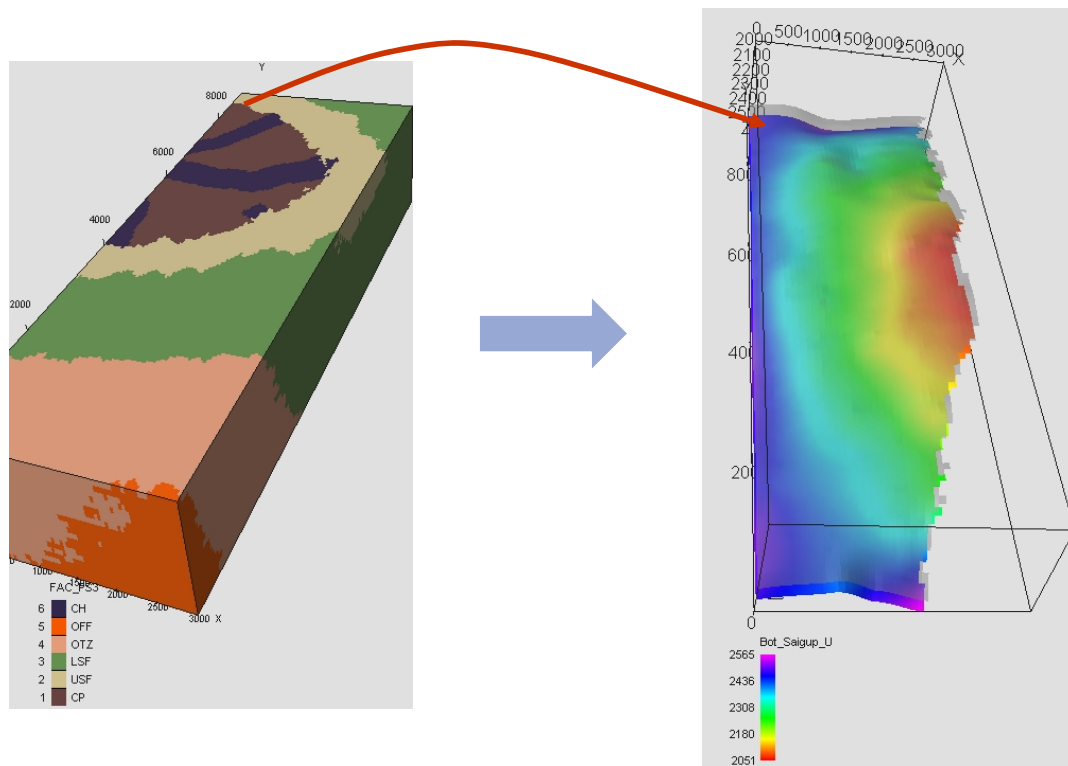
Figure 8. The mapping process from a structurally unfaulted geostatistical fine scale domain into the synthetic fine scale reservoir is shown. Each, in this case, SATNUM value is I,J,K-sampled within the zone created by the 80 meter thick difference between the structural bottom and top reservoir.

The multiplicator (MULT) values which represent the barriers were, however, not directly sampled into the fine scale grid. These were only available in the coarse scale representation, and needed, consequently, to be downscaled, without introducing holes in the barriers. Each coarse scale barrier value (MULT-value) was therefore scaled according to the ratio in resolution, for each direction. This means for instance that for a MULTX-value, which was to be downscaled by a factor 2, the square root of the value was put in both cells in the x-direction. Vertically, with a factor 4 between the grid resolutions, a value "x" was replaced by four "$x^{1/4}$"-values neighbouring each other. The process is depicted in Figure 9.
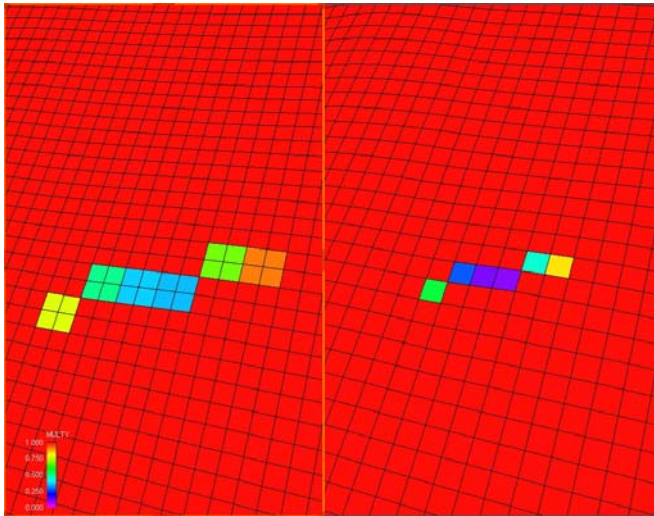
Figure 9. Downscaling MULT values. The coarse scale representation (right) produces several neighbouring cells with identical values on the fine scale representation (left). Multiplicator values (between 0 and 1) are increased since their product should become the original coarse scale value.

5   Realization index

Table 2 gives an overview on the numbering and parameter values of the input to the stochastic realizations in the synthetic suite of realizations.

Realization conversion		Sedimentological parameter					Coding numbers (Sintef)				
Sintef-real	Saigup-real	Barrier %	Lobosity	Aggra-dation	Progra-dation	Fault pattern	Bar-nr	Lob-nr	Agg-nr	Pro-nr	Fau-nr
1	89	10	Parall	Med	up-dip	U	1	1	2	1	0
2	98	50	Parall	Med	up-dip	U	2	1	2	1	0
3	107	90	Parall	Med	up-dip	U	3	1	2	1	0
4	35	10	1 lobe	Med	up-dip	U	1	2	2	1	0
5	44	50	1 lobe	Med	up-dip	U	2	2	2	1	0
6	53	90	1 lobe	Med	up-dip	U	3	2	2	1	0
7	62	10	2 lobes	Med	up-dip	U	1	3	2	1	0
8	71	50	2 lobes	Med	up-dip	U	2	3	2	1	0
9	80	90	2 lobes	Med	up-dip	U	3	3	2	1	0
10	88	10	Parall	Low	up-dip	U	1	1	1	1	0
11	97	50	Parall	Low	up-dip	U	2	1	1	1	0
12	106	90	Parall	Low	up-dip	U	3	1	1	1	0
13	34	10	1 lobe	Low	up-dip	U	1	2	1	1	0

14	43	50	1 lobe	Low	up-dip	U	2	2	1	1	0
15	52	90	1 lobe	Low	up-dip	U	3	2	1	1	0
16	61	10	2 lobes	Low	up-dip	U	1	3	1	1	0
17	70	50	2 lobes	Low	up-dip	U	2	3	1	1	0
18	79	90	2 lobes	Low	up-dip	U	3	3	1	1	0
19	90	10	Parall	High	up-dip	U	1	1	3	1	0
20	99	50	Parall	High	up-dip	U	2	1	3	1	0
21	108	90	Parall	High	up-dip	U	3	1	3	1	0
22	36	10	1 lobe	High	up-dip	U	1	2	3	1	0
23	45	50	1 lobe	High	up-dip	U	2	2	3	1	0
24	54	90	1 lobe	High	up-dip	U	3	2	3	1	0
25	63	10	2 lobes	High	up-dip	U	1	3	3	1	0
26	72	50	2 lobes	High	up-dip	U	2	3	3	1	0
27	81	90	2 lobes	High	up-dip	U	3	3	3	1	0
28	86	10	Parall	Med	down-dip	U	1	1	2	2	0
29	95	50	Parall	Med	down-dip	U	2	1	2	2	0
30	104	90	Parall	Med	down-dip	U	3	1	2	2	0
31	32	10	1 lobe	Med	down-dip	U	1	2	2	2	0
32	41	50	1 lobe	Med	down-dip	U	2	2	2	2	0
33	50	90	1 lobe	Med	down-dip	U	3	2	2	2	0
34	59	10	2 lobes	Med	down-dip	U	1	3	2	2	0
35	68	50	2 lobes	Med	down-dip	U	2	3	2	2	0
36	77	90	2 lobes	Med	down-dip	U	3	3	2	2	0
37	85	10	Parall	Low	down-dip	U	1	1	1	2	0
38	94	50	Parall	Low	down-dip	U	2	1	1	2	0
39	103	90	Parall	Low	down-dip	U	3	1	1	2	0
40	31	10	1 lobe	Low	down-dip	U	1	2	1	2	0
41	40	50	1 lobe	Low	down-dip	U	2	2	1	2	0
42	49	90	1 lobe	Low	down-dip	U	3	2	1	2	0
43	58	10	2 lobes	Low	down-dip	U	1	3	1	2	0
44	67	50	2 lobes	Low	down-dip	U	2	3	1	2	0
45	76	90	2 lobes	Low	down-dip	U	3	3	1	2	0
46	87	10	Parall	High	down-dip	U	1	1	3	2	0
47	96	50	Parall	High	down-dip	U	2	1	3	2	0
48	105	90	Parall	High	down-dip	U	3	1	3	2	0
49	33	10	1 lobe	High	down-dip	U	1	2	3	2	0
50	42	50	1 lobe	High	down-dip	U	2	2	3	2	0
51	51	90	1 lobe	High	down-dip	U	3	2	3	2	0
52	60	10	2 lobes	High	down-dip	U	1	3	3	2	0
53	69	50	2 lobes	High	down-dip	U	2	3	3	2	0
54	78	90	2 lobes	High	down-dip	U	3	3	3	2	0
55	89	10	Parall	Med	up-dip	A23	1	1	2	1	1
56	98	50	Parall	Med	up-dip	A23	2	1	2	1	1
57	107	90	Parall	Med	up-dip	A23	3	1	2	1	1
58	35	10	1 lobe	Med	up-dip	A23	1	2	2	1	1
59	44	50	1 lobe	Med	up-dip	A23	2	2	2	1	1
60	53	90	1 lobe	Med	up-dip	A23	3	2	2	1	1
61	62	10	2 lobes	Med	up-dip	A23	1	3	2	1	1
62	71	50	2 lobes	Med	up-dip	A23	2	3	2	1	1
63	80	90	2 lobes	Med	up-dip	A23	3	3	2	1	1
64	88	10	Parall	Low	up-dip	A23	1	1	1	1	1
65	97	50	Parall	Low	up-dip	A23	2	1	1	1	1
66	106	90	Parall	Low	up-dip	A23	3	1	1	1	1

NR⬡ **CO2 storage capacity subject to geological uncertainty**

67	34	10	1 lobe	Low	up-dip	A23	1	2	1	1	1
68	43	50	1 lobe	Low	up-dip	A23	2	2	1	1	1
69	52	90	1 lobe	Low	up-dip	A23	3	2	1	1	1
70	61	10	2 lobes	Low	up-dip	A23	1	3	1	1	1
71	70	50	2 lobes	Low	up-dip	A23	2	3	1	1	1
72	79	90	2 lobes	Low	up-dip	A23	3	3	1	1	1
73	90	10	Parall	High	up-dip	A23	1	1	3	1	1
74	99	50	Parall	High	up-dip	A23	2	1	3	1	1
75	108	90	Parall	High	up-dip	A23	3	1	3	1	1
76	36	10	1 lobe	High	up-dip	A23	1	2	3	1	1
77	45	50	1 lobe	High	up-dip	A23	2	2	3	1	1
78	54	90	1 lobe	High	up-dip	A23	3	2	3	1	1
79	63	10	2 lobes	High	up-dip	A23	1	3	3	1	1
80	72	50	2 lobes	High	up-dip	A23	2	3	3	1	1
81	81	90	2 lobes	High	up-dip	A23	3	3	3	1	1
82	86	10	Parall	Med	down-dip	A23	1	1	2	2	1
83	95	50	Parall	Med	down-dip	A23	2	1	2	2	1
84	104	90	Parall	Med	down-dip	A23	3	1	2	2	1
85	32	10	1 lobe	Med	down-dip	A23	1	2	2	2	1
86	41	50	1 lobe	Med	down-dip	A23	2	2	2	2	1
87	50	90	1 lobe	Med	down-dip	A23	3	2	2	2	1
88	59	10	2 lobes	Med	down-dip	A23	1	3	2	2	1
89	68	50	2 lobes	Med	down-dip	A23	2	3	2	2	1
90	77	90	2 lobes	Med	down-dip	A23	3	3	2	2	1
91	85	10	Parall	Low	down-dip	A23	1	1	1	2	1
92	94	50	Parall	Low	down-dip	A23	2	1	1	2	1
93	103	90	Parall	Low	down-dip	A23	3	1	1	2	1
94	31	10	1 lobe	Low	down-dip	A23	1	2	1	2	1
95	40	50	1 lobe	Low	down-dip	A23	2	2	1	2	1
96	49	90	1 lobe	Low	down-dip	A23	3	2	1	2	1
97	58	10	2 lobes	Low	down-dip	A23	1	3	1	2	1
98	67	50	2 lobes	Low	down-dip	A23	2	3	1	2	1
99	76	90	2 lobes	Low	down-dip	A23	3	3	1	2	1
100	87	10	Parall	High	down-dip	A23	1	1	3	2	1
101	96	50	Parall	High	down-dip	A23	2	1	3	2	1
102	105	90	Parall	High	down-dip	A23	3	1	3	2	1
103	33	10	1 lobe	High	down-dip	A23	1	2	3	2	1
104	42	50	1 lobe	High	down-dip	A23	2	2	3	2	1
105	51	90	1 lobe	High	down-dip	A23	3	2	3	2	1
106	60	10	2 lobes	High	down-dip	A23	1	3	3	2	1
107	69	50	2 lobes	High	down-dip	A23	2	3	3	2	1
108	78	90	2 lobes	High	down-dip	A23	3	3	3	2	1

Table 2. Conversion table between realizations in the CO_2 injection sensitivity study.

6 Final remarks

The symbiotic cooperation between SINTEF and NR has proven successful in this preliminary study. The CLIMIT-granted project "Impact of Realistic Geologic Models on Simulation of CO2 Storage" which will run in 2010 to 2011 will follow up on this cooperation, also together with the University of Bergen as the coordinator and CIPR as project partner.

7 Acknowledgments

8 References

Manzocchi, T., Carter, J. N., Skorstad, A., Fjellvoll, B., Stephen, K. D., Howell, J., Matthews, J. D., Walsh, J. J., Nepveu, M., Bos, C., Cole, J., Egberts, P., Flint, S., Hern, C., Holden, L., Hovland, H., Jackson, H., Kolbjørnsen, O., MacDonald, A., Nell, P. A. R., Onyeagoro, K., Strand, J., Syversveen, A. R., Tchistiakov, A., Yang, C., Yielding, G. and Zimmerman, R. W.: "Sensitivity of the impact of geological uncertainty on production from faulted and unfaulted shallow marine oil reservoirs – objectives and methods". *Petroleum Geoscience*, **Vol. 14**, No. 1, 2008.

Howell, J., Skorstad, A., MacDonald, A., Fordham, A., Flint, S., Fjellvoll, B. and Manzocchi, T.: "Sedimentological Parameterisation of Shallow Marine Reservoirs". *Petroleum Geoscience*, **Vol. 14**, No. 1, 2008.

Matthews, J. D., Carter, J. N., Stephen, K. D., Zimmerman, R. W., Skorstad, A., Manzocchi, T. and Howell, J.: "Reservoir Engineering aspects of the SAIGUP Project". *Petroleum Geoscience*, **Vol. 14**, No. 1, 2008.

Manzocchi, T., Matthews, J. D., Strand, J. A., Carter, J. N., Skorstad, A., Howell, J., Stephen, K. D. and Walsh, J. J.: "A study on the structural controls on oil recovery from shallow marine reservoir". *Petroleum Geoscience*, **Vol. 14**, No. 1, 2008**.**

Stephen, K. D., Yang, C., Carter, J. N., Howell, J., Manzocchi, T. and Skorstad, A.: "Upscaling Uncertainty Analysis in a Shallow Marine Environment". *Petroleum Geoscience*, **Vol. 14,** No. 1, 2008.